Liquid Crystals
Publication details, including instructions for authors and subscription information:
http://www.informaworld.com/smpp/title~content=t713926090

The relationship between the structures of semi-rigid homo- and copolyesters based on 5,5'-diphenyl-2,2'-bis(1,3,4-thiadiazole)s and their liquid crystalline and optical properties

Moriyuki Sato Corresponding author[a]; Miyuki Notsu[a]; Shinji Nakashima[a]
[a] Department of Material Science, Faculty of Science and Engineering, Shimane University, Matsue-shi, Shimane 690-8504, Japan

To cite this Article Sato Corresponding author, Moriyuki , Notsu, Miyuki and Nakashima, Shinji(2004) 'The relationship between the structures of semi-rigid homo- and copolyesters based on 5,5'-diphenyl-2,2'-bis(1,3,4-thiadiazole)s and their liquid crystalline and optical properties', Liquid Crystals, 31: 9, 1195 — 1205

To link to this Article: DOI: 10.1080/02678290410001720911

URL: http://dx.doi.org/10.1080/02678290410001720911

LIQUID CRYSTALS, VOL. 31, NO. 9, SEPTEMBER 2004, 1195–1205

The relationship between the structures of semi-rigid homo- and copolyesters based on 5,5′-diphenyl-2,2′-bis(1,3,4-thiadiazole)s and their liquid crystalline and optical properties

MORIYUKI SATO*, MIYUKI NOTSU and SHINJI NAKASHIMA
Department of Material Science, Faculty of Science and Engineering, Shimane University, 1060 Nishikawatsu, Matsue-shi, Shimane 690-8504, Japan

(*Received 6 November 2003; in final form 20 February 2004; accepted 10 March 2004*)

New semi-rigid homo- and copolyesters composed of the quaterphenyl analogue of 2,2′-bis(1,3,4-thiadiazole) (BTD), 5,5′-diphenyl-2,2′-bis(1,3,4-thiadiazole) (DBTD), were prepared by high temprature solution polycondensation of monomers, 3,3′- and 4,4′-dioxydiundecanol derivatives of DBTD with four dimethyl esters, and their liquid crystalline (LC) and optical properties were investigated. DSC measurements, texture observations using a polarizing microscope equipped with a hot stage, and powder X-ray diffraction showed that the homopolymers containing the 4,4′-DBTD unit form more stable LC phases than those having the 3,3′-DBTD unit. The 4,4′-DBTD-containing polymers and the 3,3′-DBTD unit-poor copolymers, except for the 3,3′-DBTD unit-rich copolymers and the 3,3′-DBTD-containing homopolymers (which formed highly ordered smectic or crystal mesophases), displayed a thermotropic LC smectic C phase. Solution and solid state UV-vis and photoluminescent (PL) spectra showed that the polyesters display miximum absorbances and bluish-green or blue emission based on the DBTD unit, where the Stokes shifts were observed. The peak positions in the UV-vis and the PL spectra of homopolymers composed of the 4,4′-DBTD unit were at higher wavelengths than those in the corresponding 3,3′-DBTD-containing homopolymers, due to its more conjugated structure. In the copolymers the peak maxima were shifted to shorter wavelengths with the increase of 3,3′-DBTD content.

1. Introduction

It is well known that low molar mass compounds, oligomers and polymers consisting of heterocyclic units such as thiophenes, 1,3,4-oxadiazoles and 1,3,4-thiadiazoles are charge-transporting and/or light-emitting materials with application potential in organic electroluminescent (EL) devices, and thus have attracted much attention as materials for use in the next generation of such technologies [1–10].

Thermotropic LC polymers containing calamitic mesogens such as biphenyl, diphenyls and heterocyclic units in the main chain, have unique properties arising from the orientational ordering in their mesophase; their LC properties depend on various structural factors: mesomorphic properties of the calamitic mesogen, linearity and rigidity of the polymer chain, intermolecular interactions, copolymer composition, etc. [11–15]. The mesomorphic tendency of heterocyclic mesogens decreases in the order [15].

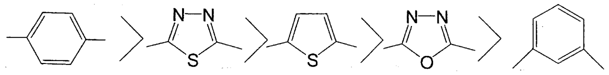

In our previous work, a series of main chain semi-rigid polymers [16–22] and low molar-mass compounds [23, 24] composed of biphenyl [16, 17], terphenyl [18, 19], quaterphenyl [20], quinquephenyl [21] and distyrylbenzene analogues [22] of 1,3,4-thiadiazole (which is a five-membered heterocyclic moiety analogous to 1,3,4-oxadiazole and a good mesogen) were prepared and their LC, photoluminescent (PL) and EL properties investigated. Among them, the quaterphenyl analogue of 2,2′-bis(1,3,4-thiadiazole) (BTD), 5,5′-diphenyl-2,2′-bis(1,3,4-thiadiazole (DBTD) [24], and semi-rigid homopolyesters [20] comprising the DBTD unit, were found not only to show smectic and/or nematic phases, but also to display PL and EL properties with light emission, and behaved as electron-transporting and light-emitting materials. These were suggested to be candidate materials for organic EL devices, although they crystallize and aggregate during the measurements of EL properties. Very recently we prepared thermotropic LC semi-rigid

*Author for correspondence;
e-mail: msato@riko.shimane-u.ac.jp

Liquid Crystals ISSN 0267-8292 print/ISSN 1366-5855 online © 2004 Taylor & Francis Ltd
http://www.tandf.co.uk/journals
DOI: 10.1080/02678290410001720911

polyesters based on three terphenyl analogues of 1,3,4-thiadiazole (2,5-diphenyl-1,3,4-thiadiazole, DPTD) linking the undecamethyleneoxy chain at different substitution positions, and showed that polyesters composed of the DPTD unit having a more linear molecular structure and a 1,4-phenylene unit or short aliphatic chain tend to form smectic C and/or A phases [19]. The mesomorphic tendency of the polyesters decreased and the peak maxima in their absorption and emission spectra were shifted to lower wavelengths in the following order: 4,4′-DPTD > 3,4′-DPTD > 3,3′-DPTD.

In this article, semi-rigid homo- and copolyesters **7a–d** and **8a–d** containing the quaterphenyl analogue of BTD (DBTD) in the main chain were prepared from the two diol monomers **5a** and **5b** based on DBTD and having undecamethyleneoxy chains at different (4,4′- and 3,3′-disubstituted) positions, and the dimethyl esters **6a–d**, by high temperature solution polycondensation. The relationships between the polymer structures and the LC and PL properties were investigated in order to develop of polymeric materials with improved thermal and optical characteristics for use in the organic EL devices.

2. Experimental

The various steps in the synthesis of compounds **7a–d** and **8a–d** are illustrated in schemes 1–3.

2.1. *Materials*

3-Methoxybenzoyl chloride **1a**, oxalyl dihydrazide **2**, Lawesson's reagent, hydrobromic acid, 11-bromoundecanol, potassium carbonate and 1,4-dioxane were commercially available and used as received.

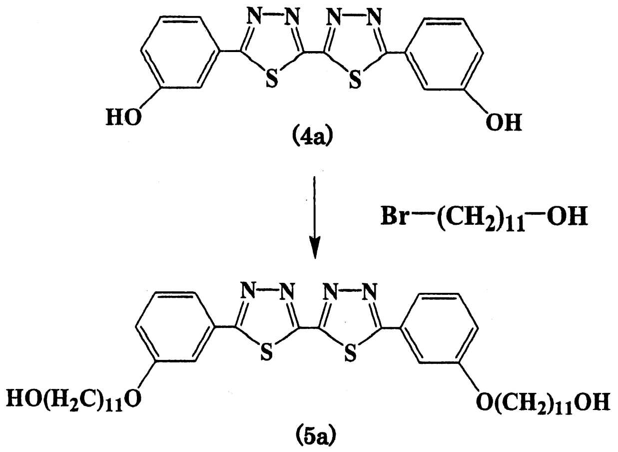

Scheme 1.

1-Chloronaphthalene (special grade) was used after drying. Pyridine, dichloroacetic acid (DCAA), trifluoroacetic acid (TFAA), 1,1,1,3,3,3-hexafluoroisopropanol (HFIP), *N*,*N*-dimethylacetamide (DMAc) and *N*,*N*-dimethylformamide (DMF) were purified by vacuum distillation. Dimethly adipate **6a**, dimethyl sebacate **6b**, dimethyl isophthalate **6c** and dimethyl terephthalate **6d** were used after purification. 5,5′-Bis[4-(11-hydroxyundecyloxy)phenyl]-2,2′-bis(1,3,4-thiadiazole) **5b** was prepared according to our published method [20].

2.2. *Synthesis of monomers*

2.2.1. *5,5′-Bis(3-methoxyphenyl)-2,2′-bis(1,3,4-thiadiazole) 3a*

3-Methoxybenzoyl chloride **1a** (0.1 mol, 17.1 g) was dissolved in DMAc (30 ml) in the presence of pyridine (0.1 mol. 7.91 g) at 0–10°C. Oxalyl dihydrazide **2**

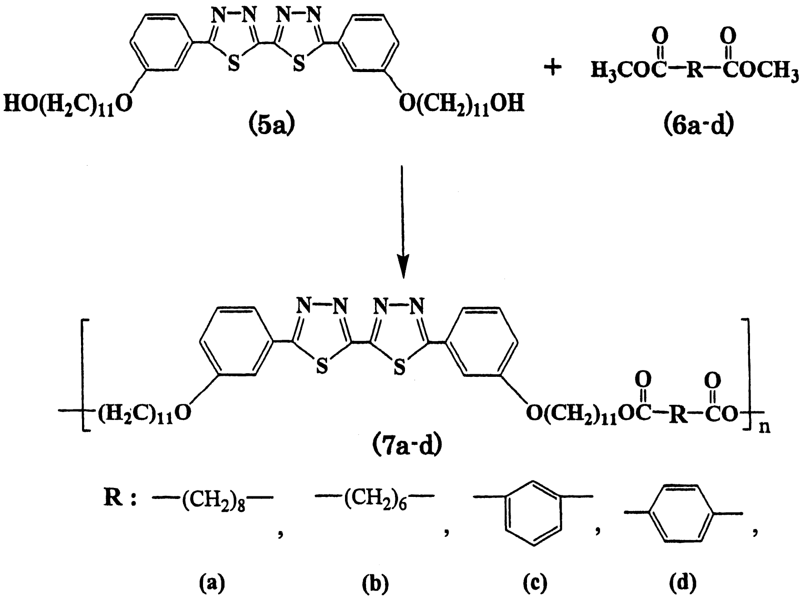

Scheme 2.

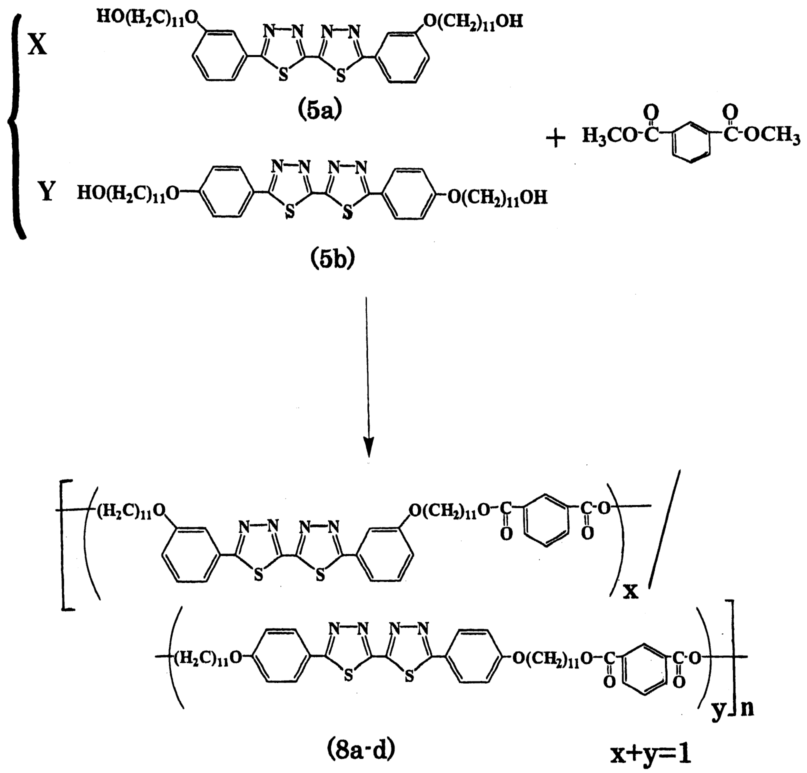

Scheme 3.

(0.05 ml, 5.90 g) and DMAc (100 ml) in limited amounts were added to the solution cooled in an ice-water bath. The mixture was stirred below 10°C for 2.5 h; it was then held at ambient temperature for 20 h and heated at 80°C for an additional 2.5 h. After the reaction was completed, the solution was cooled and poured into water to precipitate the intermediate dihydrazide compound **3a–id**. 1M HCl was added to the mixture and excess DMA and pyridine were removed by neutralization. The solid obtained was filtered off, washed thoroughly with water and dried at 60°C for several days. The intermediate dihydrazide compound **3a–id** (0.0259 mol, 7.78 g) was then heated under refluxed in 1,4-dioxane (100 ml) in the presence of Lawesson's reagent (62.2 mmol, 25.1 g) for 3.5 h. A yellow solid precipitated during the cyclodehydration. After completion of the reaction, the mixture was poured into an excess of 1M NaOH containing ice and held at room temperature. The precipitated solid was filtered off and washed thoroughly with water and methanol over night. The resulting product **3a** was recrystallized from DMAc and dried at 60°C for a day under vacuum; yield 79%, m.p. 238°C (DSC method). Elemental analysis for $C_{18}H_{14}N_4O_2S_2$ (382.4): calc. C 56.53, H 3.69, N 14.65%; found C 56.02, H 3.72, N 14.69%. FTIR (KBr disk): $\nu = 1595$ (s, C=N), 1580 (shoulder, C=C), 1419 (s, 1,3,4-thiadiazole), 1267 cm^{-1} (s, C–O–C).

2.2.2. *5,5′-Bis(3-hydroxyphenyl)-2,2′-bis(1,3,4-thiadiazole)* ***4a***

The dimethoxy compound **3a** (10.4 mmol, 39.8 g) was heated under reflux in a mixture of acetic acid (50 ml) and hydrobromic acid (270 ml) for 24 h. The mixture was poured into an excess of water. The precipitate was collected by filtration and dissolved in 2M aqueous NaOH, which was then acidified with acetic acid to precipitate the product. The precipitated solid was filtered off and washed thoroughly with water. Compound **4a** was recrystallized from DMF and dried at 60°C for 24 h under vacuum; yield 96%, m.p. >300°C. Elemental analysis for $C_{16}H_{10}N_4O_2S_2$ (354.4): calc. C 54.22, H 2.84, N 15.81; found C 53.87, H 3.11, N 15.79%. FTIR (KBr disk): $\nu = 3190$ (m, OH stretching), 1620 (shoulder, C=N), 1595 (m, C=C), 1425 cm^{-1} (s, 1,3,4-thiadiazole).

2.2.3. *5,5′-Bis[3-(11-hydroxyundecyloxy)phenyl]-2,2′-bis(1,3,4-thiadiazole)* ***5a***

As indicated in scheme 1, a mixture of the dihydroxy compound **4a** (4.14 mmol, 1.47 g), 11-bromoundecanol (8.49 mmol, 2.13 g) and potassium carbonate

(8.49 mmol, 1.17 g) was heated in refluxing DMF for 24 h under nitrogen. After completion of the reaction, the mixture was poured into water to precipitate the product; it was filtered off and washed thoroughly with water and methanol. The resulting compound **5a** was recrystallized from DMF twice and dried at 60°C under vacuum for 1 d; yield 57%, m.p. Cr 148°C S 154°C I. Elemental analysis for $C_{38}H_{54}N_4O_4S_2$ (694.9): calc. C 65.67, H 7.82, N 8.06; found C 64.59, H 7.25, N 8.19%. FTIR (KBr disk): $v = 3350$ (m, OH stretching), 2920, 2850 (s, CH stretching), 1598 (s, C=N and C=C), 1423 (s, 1,3,4-thiadiazole), 1267 cm^{-1} (s, C–O–C). ^1H NMR ($DCAA/CDCl_3 = 3/1$ v/v): $\delta = 7.1$–7.6 (m, 8H, aromatic protons), 4.05–4.12 (t, 4H, OCH_2), 3.93 (s, 2H, OH), 3.7–3.8 (t, 4H, CH_2OH), 1.2–1.9 ppm (m, 28H, aliphatic CH_2).

2.3. *Synthesis of Homopolymers* ***7a–d***

A typical procedure for preparation of homopolyester **7c** is described, see scheme 2. Monomer **5a** (0.36 mmol, 0.250 g), dimethyl isophthalate **6c** (0.36 mmol, 0.0699 g), di-*n*-butyltin oxide (5 mg) as catalyast and 1-chloronaphthalene (2 ml) as solvent were placed in a flask and the mixture heated at 190°C with stirring under nitrogen for 12 h. The byproduct, methanol was removed from the reaction system every 1 h. After the polycondensation, the product was dissolved in TFAA (2 ml) and the solution poured into methanol to precipitate the polymer. The solid obtained was filtered off, washed thoroughly with water and three times with refluxing methanol. Drying at 60°C for 24 h under vacuum gave the expected polymer **7c**; yield 84%.

2.4. *Synthesis of Copolymer* ***8a–d***

As indicated in scheme 3, a mixture (0.36 mmol) of monomers **5a** and **5b** was taken in a definite mole ratio with dimethyl isophthalate **6c** (0.36 mmol), and polycondensed at 190°C in 1-chloronaphthalene (2 ml) in the presence of di-*n*-butyltin oxide (5 mg) as catalyst, according to the above-described method for the preparation of homopolymer **7c**. After polymerization, the copolymer obtained was purified and dried by the same procedure; yield 82–88%.

2.5. *Measurements*

^1H NMR spectra were recorded with a JEOL LMN EX270 spectrometer in $DCAA/CDCl_3 = 1/3$ v/v. FTIR spectra were obtained on a Jasco FTIR 5300 spectrometer by the KBr disk method. Differential scanning calorimetry (DSC) measurements were carried out with a Shimadzu DSC-60 calorimeter at heating and cooling rates of 10°C min^{-1} under nitrogen. Polarizing microscopy of textures was performed with a polarizing microscope (Nikon) equipped with a hot plate (magnification × 200). Powder X-ray analyses at room temperature were undertaken by a Rigaku Denki RINT 2500 generator with CuK_α irradiation. UV-vis and the PL spectra were measured on a Jasco V-560 UV/VIS spectrometer or a Shimadzu UV-vis 3100 spectrometer and on a Hitachi 850 fluorescence spectrophotometer, respectively. Inherent viscosity measurements were conducted at a concentration of 0.2 g dl^{-1} in DCAA at 30°C using an Ostwald type viscometer.

3. Results and discussion

3.1. *Polymer syntheses*

In a previous communication [20], we reported the preparation of semi-rigid thermotropic LC polyesters containing the quaterphenyl analogue of BTD (DBTD) from the 4,4′-dioxydiundecanol derivative **5b** of DBTD and four diacyl chlorides, and found that they show both LC and PL properties, similar to the semi-rigid polyesters composed of the DPTD unit [18, 19].

In this work, four semi-rigid homopolyesters **7a–d** composed of the 3,3′-disubstituted DBTD unit were prepared by high temperature polycondensation of the 3,3′-dioxydiundecanol derivative of DBTD **5a** with four dimethyl esters **6a–d** in the presence of di-*n*-butyltin oxide as catalyst in 1-chloronaphthalene (see scheme 1). The copolyesters **8a–d**, having different disubstituted (3,3′- and 4,4′-) DBTD units in the main chain, were synthesized from a mixture of two dioxydiundecanol (3,3′- and 4,4′-) derivatives **5a** and **5b**, taken in a definite mole ratio, and dimethyl isophthalate **6c**, see scheme 3. The structures of polyesters **7a–d** and **8a–d** were characterized by FTIR and ^1H NMR spectroscopies, and elemental analyses. The monomer, i.e. the 3,3′-dioxydiundecanol derivative **5a** of DBTD, was prepared from the 3,3′-dihydroxy derivative **4a** of DBTD (which was synthesized by heating the corresponding 3,3′-dimethoxy derivative **3a** in hydrobromic acid and 11-bromoundecanol by the Williamson reaction in the presence of potassium carbonate in DMF, according to our previously reported method [20] for the 4,4′-dioxydiundecanol derivative **4b** of DBTD, as shown in scheme 1.

The characterization data for polymers **7a–d** and **8a–d** are listed in table 1. The polyesters **7a–d** and **8a–d** were soluble in organic solvents such as TFAA and DCAA at room temperature, but insoluble in, for example, chloroform and methanol. Inherent viscosities of the polymers **7a–d** and **8a–d**, measured at a concentration of 0.2 g dl^{-1} in DCAA at 30°C, were 0.16–0.30 dl g^{-1}. The FTIR spectra of the polyesters contained characteristic absorption bands of the ester

Table 1. Yields, inherent viscosities and elemental analysis data for polymers **7a**–**d** and **8a**–**d**.

Polymer	x	y	Yield/%	$\eta_{inh}{}^{a}$/dL g^{-1}	Elemental Formula (formula wt.)		Elemental analysis/% C	H	N
7a	1.0	0	84	0.16	$(C_{48}H_{68}N_4O_6S_2)_n$	Calc.	66.95	7.96	6.51
					$(861.1)_n$	Found	65.45	7.52	6.34
7b	1.0	0	82	0.18	$(C_{46}H_{64}N_4O_6S_2)_n$	Calc.	66.31	7.74	6.73
					$(833.0)_n$	Found	64.73	7.28	6.58
7c	1.0	0	84	0.18	$(C_{46}H_{56}N_4O_6S_2)_n$	Calc.	66.96	6.84	6.79
					$(823.0)_n$	Found	65.64	6.52	6.84
7d	1.0	0	53	0.17	$(C_{46}H_{56}N_4O_6S_2)_n$	Calc.	66.96	6.84	6.79
					$(823,0)_n$	Found	65.48	6.56	6.34
8a	0.8	0.2	88	0.25	$(C_{46}H_{56}N_4O_6S_2)_n$	Calc.	66.96	6.84	6.79
					$(823.0)_n$	Found	65.83	6.58	6.92
8b	0.6	0.4	84	0.26	$(C_{46}H_{56}N_4O_6S_2)_n$	Calc.	66.96	6.84	6.79
					$(823.0)_n$	Found	65.58	6.53	6.79
8c	0.4	0.6	82	0.27	$(C_{46}H_{56}N_4O_6S_2)_n$	Calc.	66.96	6.84	6.79
					$(823.0)_n$	Found	65.73	6.56	6.80
8d	0.2	0.8	86	0.30	$(C_{46}H_{56}N_4O_6S_2)_n$	Calc.	66.96	6.84	6.79
					$(823.0)_n$	Found	66.06	6.57	6.84

[a]Measured at a concentration of 0.2 g dL^{-1} in DCAA at 30°C.

C=O at 1720–1735 cm^{-1}, the C=C of the benzene ring near 1600 cm^{-1}, the thiadiazole unit around 1420 cm^{-1}, C–O–C at 1240–1270 cm^{-1}, and CH stretching around 2820–2920 cm^{-1}. The ^{1}H NMR spectra of polymers **7a**–**d** and **8a**–**d** measured in DCAA/CDCl$_3$ = 1/3 v/v revealed proton signals for OCH$_2$ and CH$_2$OC(O) around 4.12 ppm, OC(O)CH$_2$ at 2.41 ppm, aromatic protons at 7.18–7.60 ppm, aliphatic chains at 1.25–1.90 ppm and terminal CH$_2$OH around 3.80 ppm. The elemental analysis results for polyesters **7a**–**d** and **8a**–**d** agreed with calculated values. From these data, the preparations of the polyesters **7a**–**d** and **8a**–**d** were confirmed.

3.2. *Thermotropic LC properties of polyesters 7a–d and 8a–d*

Our previous articles [18–20] described the formation of thermotropic LC (smectic and nematic) phases by semi-rigid polyesters composed of the DPTD and 4,4′-disubstituted DBTD moieties. In this paper thermotropic LC properties of homopolyesters **7a**–**d** and copolyesters **8a**–**d** having the 3,3′-disubstituted unit and polymers **9a**–**d** (see scheme 4) having the 4,4′-disubstituted DBTD units were evaluated by means of differential scanning calorimetry (DSC), texture observations using a polarizing microscope equipped with a hot stage and powder X-ray analyses.

The DSC traces of homopolymers **7a**–**d** for the second heating runs and polymers **7c** and **8a** for the first cooling scans are shown in figures 1 and 2, respectively. Phase transition temperatures and associated thermodynamic data of the polymers **7a**–**d** and **8a**–**d** are listed in table 2. In the DSC traces of polymers **7a**, **7b** and **7d** on the second and the first heating scans, two or three endotherms due to solid–solid (T_{Cr}) at 115–122°C, solid–LC phase (T_m) at 122–148°C and LC phase–isotropic (T_i) transitions at 160–176°C are observed. On the first cooling scan, the corresponding exotherms based on anisotropization (T_i), LC phase–solid transition (T_c) and T_{Cr} were detected. Polarizimg microscopy indicated that polymers **7a**, **7b** and **7d** form enantiotropic fine textures in the range between T_m (T_c)

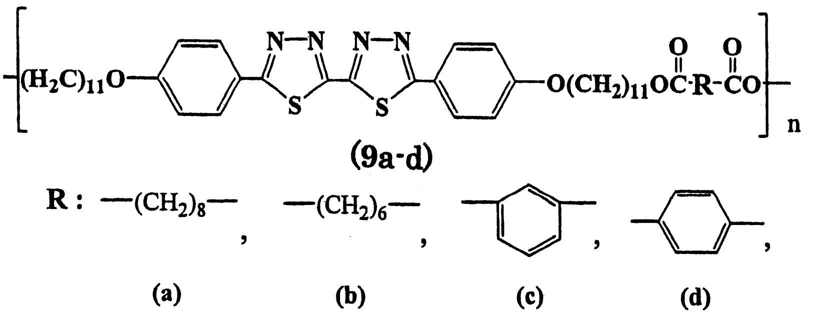

Scheme 4.

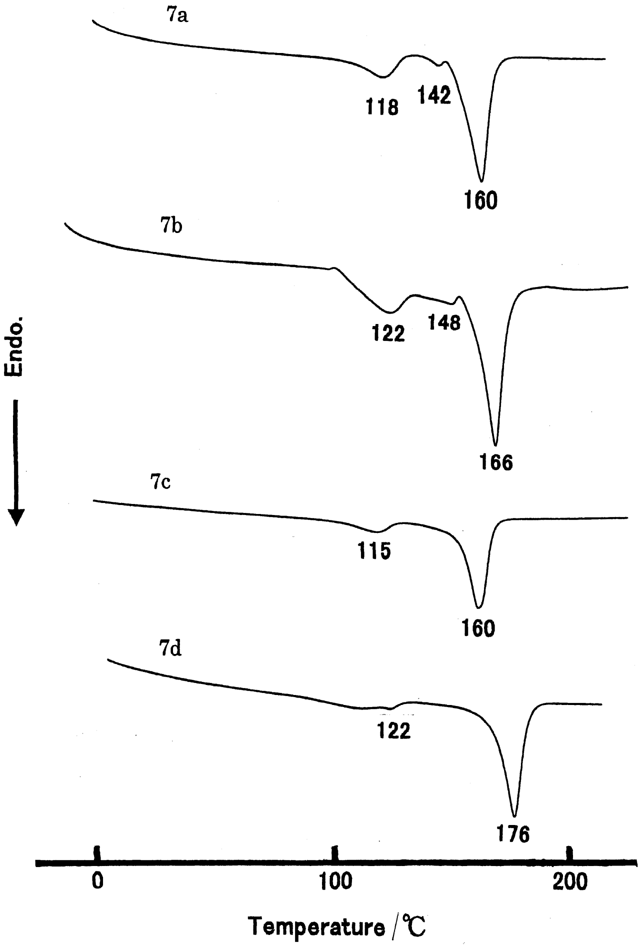

Figure 1. DSC traces for polymers **7a–d** obtained on the second heating runs.

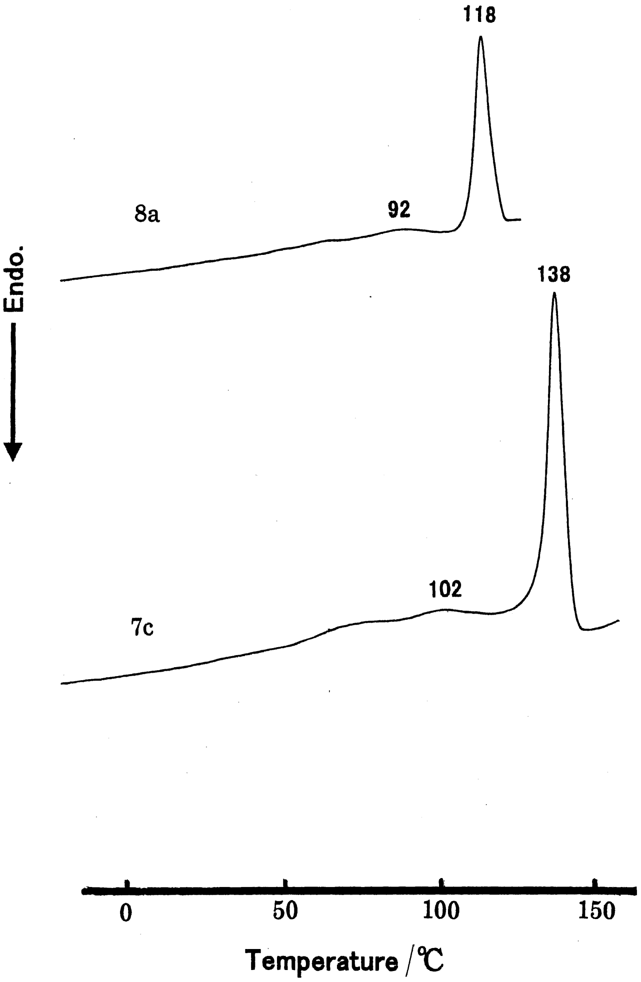

Figure 2. DSC traces for polymers **7c** and **8a** obtained on the first cooling runs.

Table 2. Phase transition temperatures and thermodynamic data for polymers **7a–d** and **8a–d**[a].

Polymer	T_g/°C	T_{Cr}/°C	T_c/°C	ΔH_c/J g^{-1}	T_m/°C	ΔH_m/J g^{-1}	T_i/°C	ΔH_i/J g^{-1}	ΔT/°C
7a	—	118	—	—	142	0.62	160	38.5	18
7b	—	122	—	—	148	1.66	166	35.6	18
7c	—	—	115,	—	160	—	—	—	—
7c[b]	—	—	(102)	(1.22)	—	—	(138)[c]	(40.5)	(36)
7d	—	—	—	—	122	0.38	176	36.5	54
8a	56	134	141	—	158	—	—	—	—
8a[b]	—	—	(92)	(1.69)	—	—	(118)[c]	(24.1)	(26)
8b	—	137,150	—	—	163	5.17	203[d]	<0.52	40
8c	—	148	154	—	166	7.35	250	0.52	84
8d	—	137	—	—	164	3.22	260	0.52	96
9c[e]	—	90	—	—	138	12.0	267	13.9	129

[a] Observed on the second heating scan (enantiotropic phase); T_g = glass transition temperature, T_{Cr} = solid-to-solid transition temperature, T_c = crystallization temperature, T_m = solid-to-smectic phase transition temperature, T_i = isotropization temperature; $\Delta T = T_i - T_m$ or $T_i - T_c$ (temperature range of mesophase).
[b] On the first cooling scan (monotropic phase).
[c] Anistropization temperature.
[d] By the polarizing microscopy.
[e] Previously reported data [20].

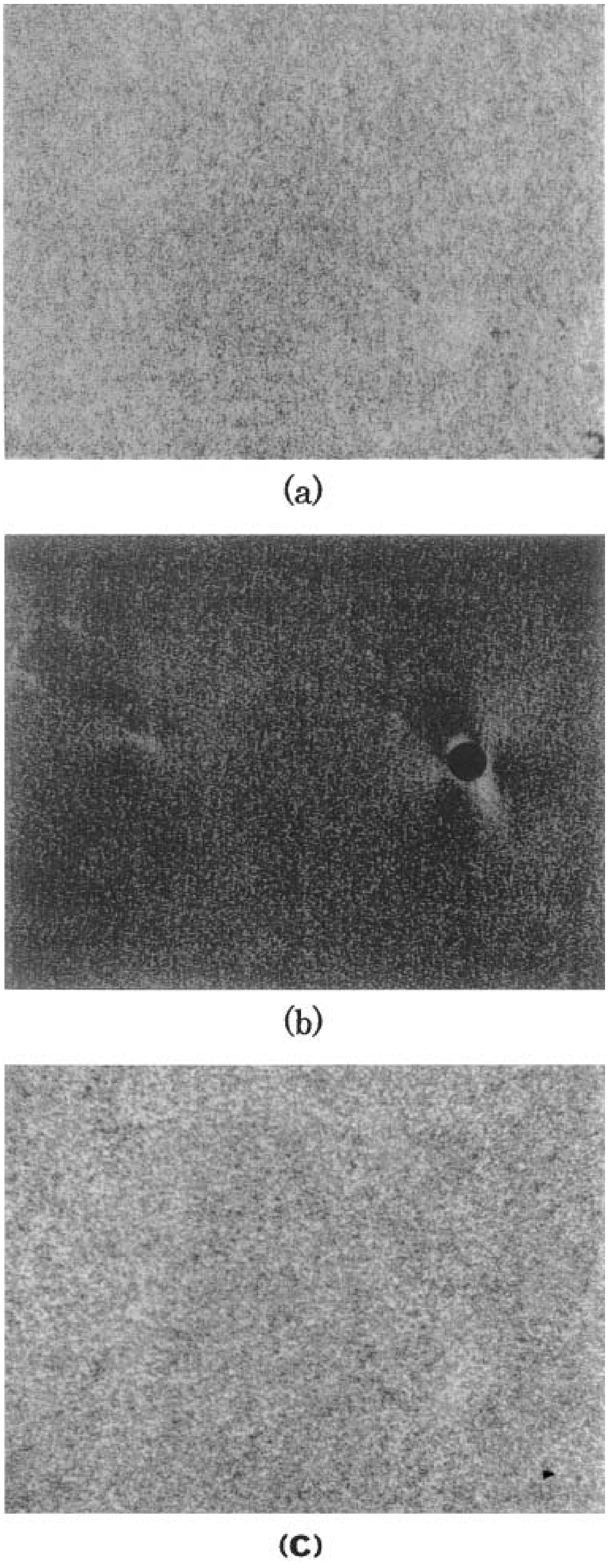

Figure 3. Polarizing photomicrographs of polymers **7b**, **8a** and **8c** (magnification × 200): (*a*) polymer **7b** at 155°C on heating, (*b*) polymer **8a** at 116°C on cooling, (*c*) polymer **8c** at 173°C on heating.

and T_i on heating or cooling. Typical polarizing photomicrograph of polymer **7b** at 155°C on heating is shown in figure 3 (*a*). The DSC trace of polymer **7c** showed two endothermic peaks due to T_{Cr} at 115°C and a normal melting transition at 160°C on the heating runs, but on cooling three exotherms including anisotropization (T_i) at 138°C, and T_c at 102°C. Polarizing microscopy showed that the polymer **7c** exhibits spherulitic texture between T_{Cr} and T_m on heating, but forms a monotropic fine texture between the T_i and T_c on cooling. The LC temperature ranges of polymers **7a–d** are 18–54°C, narrower than those of the corresponding polymers composed of the 4,4′-DBTD unit. Transition enthalpies of polymers **7a–d** are 35.6–40.5 J g^{-1} (ΔH_i) for T_i, 0.38–1.66 J g^{-1} (ΔH_m) for T_m and 1.22 J g^{-1} (ΔH_c) for T_c.

In the DSC traces of copolyesters **8a–d** for the second and first heating runs, two or more endotherms due to T_{Cr} at 134–150°C, T_m at 158–166°C and T_i transitions at 203–260°C were observed. In the first cooling runs, the corresponding exotherms (T_i, T_c and T_{Cr}) were detected. Polarizing microscopy revealed that copolymers **8b–d** show an enantiotropic LC phase (fine texture) between T_m (T_c) and T_i on heating and cooling; but the 3,3′-unit rich copolymer **8a** forms a monotropic fine texture in the range between T_c, 92°C, and the anistropization temperature T_i, 118°C, on cooling (figure 2) like the homopolymer **7c**. The polarizing photomicrograph of polymer **8a** at 116°C obtained on cooling is shown in figure 3 (*b*). The LC temperature ranges (26–84°C) of the copolyesters **8a–d** changed with composition and became narrower with increasing amounts of the 3,3′-DBTD unit. The phase transition enthalpies of copolymers **8a–d** are 3.22–7.35 J g^{-1} (ΔH_m) for T_m, 1.69 J g^{-1} (ΔH_c) for T_c and 0.52–24.1 J g^{-1} (ΔH_i) for T_i.

The LC phases of the homopolymers **7a–d** and the copolymers **8a–d** as well as the previously reported polyesters **9a–d** [20] (scheme 4) composed of the 4,4-disubstituted DBTD, were quenched from the LC phase between T_m (T_c) and T_i, and characterized at room temperature by powder X-ray diffraction. The X-ray diffraction patterns of homopolymers **7a–d** shown in figure 4 consist of two sharp reflections at small angles (the first order reflection at $2\theta = 2.18$–$2.96°$ and a second order reflection at $2\theta = 4.55$–$6.08°$), reflections at middle angles ($2\theta = 14°$) and some reflections at wide angles ($2\theta = 23$–$25°$). *d*-Spacings estimated from the X-ray analysis data of polymers **7a–d** are 29.9–40.6 Å, see table 3. The first and the second order reflections at small angles suggest the formation of a smectic phase by the polymers **7a–d**. In general, some reflections at wide angles together with the sharp reflections at small angles indicate the formation of a higher ordered

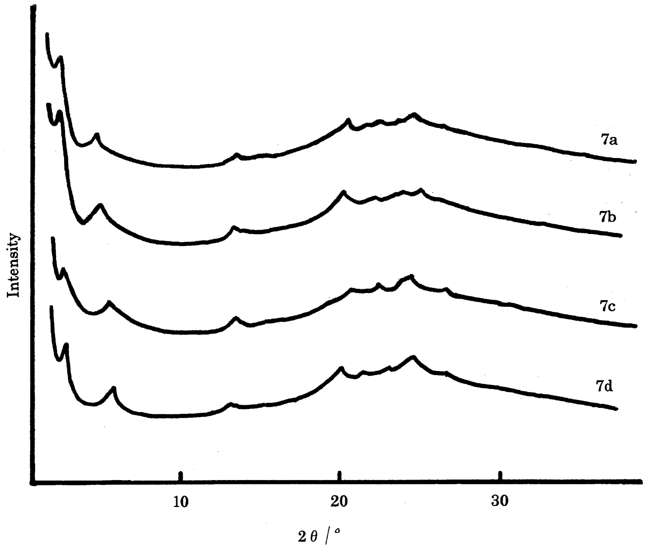

Figure 4. Powder X-ray patterns for polymers **7a–d**.

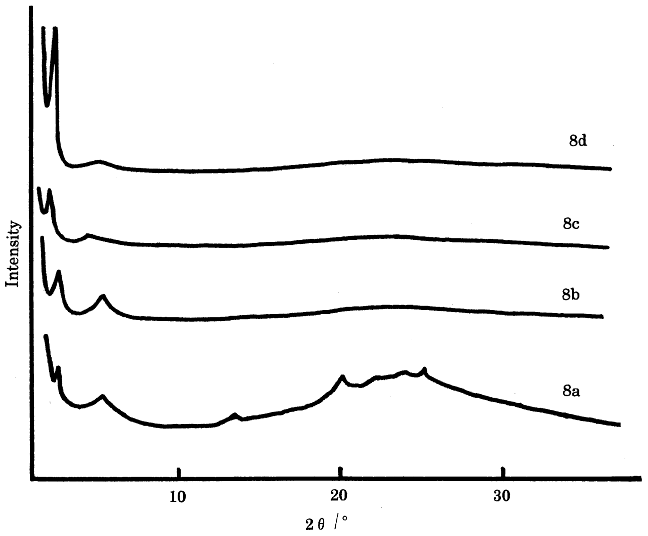

Figure 5. Powder X-ray patterns for polymers **8a–d**.

smectic phase or a crystal phase (solid smectic B, E, G or H phase). Therefore, in the present cases, the reflections at middle angles of around $2\theta = 14°$, in addition to the reflections at wide angles of $2\theta = 23–25°$ and at small angles of $2\theta = 2.18–2.96°$ and $4.55–6.08°$, are considered to be due to the formation of a highly ordered smectic or crystal phase (F, G or H phase).

In the X-ray patterns of copolymers **8a–d** shown in figure 5, the copolymers **8b–d** show two sharp (first and second order) reflections at small angles at $2\theta = 2.22–2.74°$ and $4.52–5.46°$ and broad reflections at wide angles ($2\theta = 20–30°$), which are typical X-ray patterns indicating the formation of a frozen smectic C or A phase. As shown in table 3, the estimated *d*-spacing values are 32.3–39.8 Å. Therefore, the LC phase of polymers **8b–d** is assigned as the frozen smectic C phase. In the copolymer **8a** an X-ray pattern analogous to those of the polymers **7a–d** was observed, in which the reflections at middle ($2\theta = 13°$) and wide angles ($2\theta = 22–25°$) together with sharp reflections at small angles ($2\theta = 2.73°$ and $5.53°$) were seen. This suggests the formation of a highly ordered smectic or crystal phase (F, G or H phase) in the copolymer **8a** as with as the homopolymers **7a–d** composed of the 3,3′-DBTD unit. These X-ray data indicate that the copolymers **8a–d** form a frozen smectic phase or a highly ordered smectic crystal phase (F, G or H Phase) despite the presence of two different disubstituted DBTD units in the polymer chains.

The homopolymers **9a–d**, containing the 4,4′-DBTD unit, give X-ray patterns (figure 6) consisting of one or two sharp reflections at small angles, the first order reflection at $2\theta = 1.88–2.59°$ and a second order reflection at $2\theta = 4.72–5.30°$, together with broad

Table 3. X-ray data for polymers **7a–d** and **8a–d**[a].

Polymer	2θ/°	*d*-Spacing/Å	Molecular length[b]/Å	Mesophase
7a	2.18, 4.55	40.6, 19.4	60.2	Higher ordered smectic
7b	2.30, 4.62	38.4, 19.1	57.6	Higher ordered smectic
7c	2.56, 5.27	34.5, 16.8	53.9	Higher ordered smectic
7d	2.96, 6.08	29.9, 14.5	53.7	Higher ordered smectic
8a	2.73, 5.53	32.3, 16.0	—	Higher ordered smectic
8b	2.74, 5.46	32.3, 16.2	—	Frozen smectic C
8c	2.22, 4.52	39.8, 19.5	—	Frozen smectic C
8d	2.38, 4.84	37.0, 18.2	—	Frozen smectic C
9a	1.88	47.0	60.5	Frozen smectic C
9b	2.25, 5.21	39.2, 17.0	57.7	Frozen smectic C
9c	2.26, 4.72	39.1, 18.7	54.1	Frozen smectic C
9d	2.59, 5.30	34.1, 16.7	53.9	Frozen smectic C

[a] Quenched from the LC state between $T_m(T_c)$ and T_i.
[b] Repeat unit of polymer.

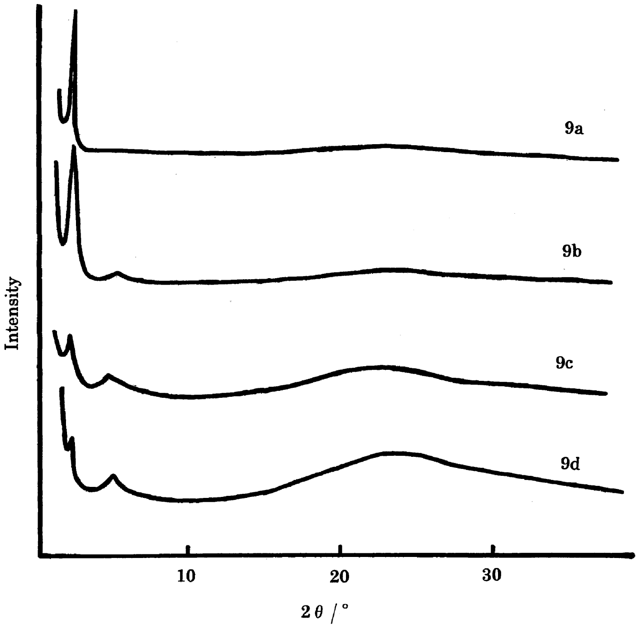

Figure 6. Powder X-ray patterns for polymers **9a–d**.

reflections at wide angles at $2\theta = 20$–$30°$. The estimated *d*-spacing values are 34.1–47.0 Å, which are shorter than the molecular lengths of the polymer repeat unit (53.9–60.5 Å) (table 3). The homopolymers **9a–d**, containing the 4,4′-DBTD moiety in the main chain, form smectic C phase as with the copolymers **8b–d**.

From these observations, it is suggested that the stability of the LC phase in the polymers **7a–d** and **8a–d**, composed of the 3,3′-DBTD unit, is lower than that in the polyesters **9a–d** having the 4,4′-DBTD unit, similar to the behaviour previously of the reported polyesters composed of the 4,4′-, 3,4′- or 3,3′-DPTD units [18, 19]. This means that the potential of the 4,4′-DBTD unit for LC formation in polymers is higher than that of 3,3′-DBTD unit. This is probably due to the fact that the 3,3′-DBTD unit has a more non-linear molecular structure than the 4,4′-DBTD moiety. Interestingly, the 3,3′-DBTD-containing polymers tend to form higher ordered smectic phases. This may reflect that they have more chain-packed molecular structures, which promote the formation of the higher ordered smectic-like phases, compared with the 4,4′-DBTD unit-containing polymers. Molecular models of the polymers **7d** and **9d** show that the molecular chain of polymer **7d** is more linear than that of polymer **9d** despite the more bent molecular structure of the 3,3′-DBTD moiety. Thus, 3,3′-DBTD supports the formation of higher ordered smectic phases by the molecular orientation and chain packing in the polymers **7a–d**.

3.3. *Optical properties of polyesters **7a–d** and **8a–d***

UV-vis and photoluminescent spectra of the polyesters **7a–d** and **8a–d** were measured in HFIP solution and in the solid state. The UV-vis spectra of homopolymers **7a–d** in the solutions were normalized to absorption peak maxima at 329.5–331.5 nm based on the $\pi-\pi^*$ electron transition of the BTD unit, but the polymers **7a–d** exhibited no PL spectra in HFIP solution on excitation at 329.5–331.5 nm, despite the generation of PL light with bluish-green emission in the analogous 4,4′-DBTD-containing polymers **9a–d**.

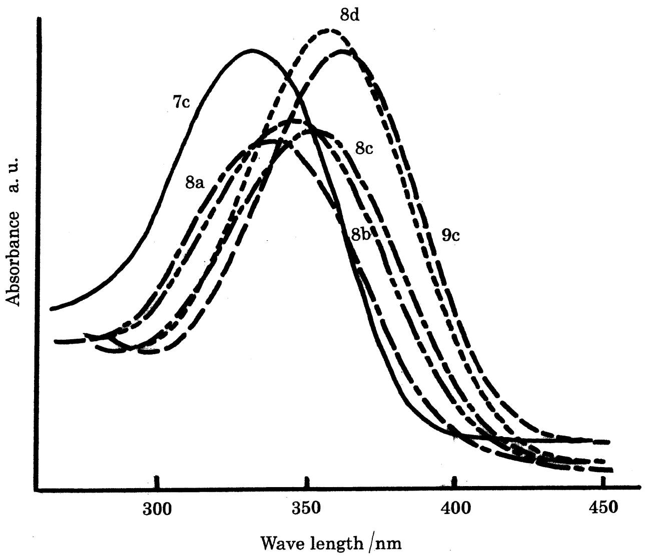

Figure 7. Solution UV-vis spectra for polymers **7c**, **8a–d** and **9c**.

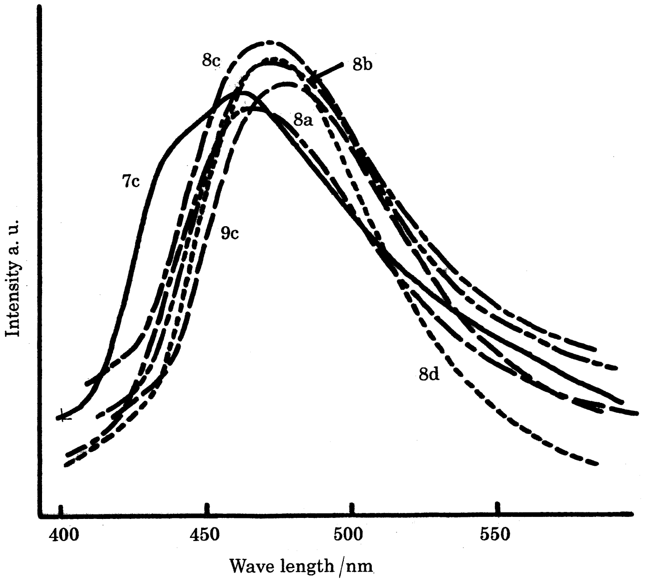

Figure 8. Solid state PL spectra for polymers **7c**, **8a–d** and **9c**.

Table 4. UV-vis and PL spectral data for polymers **7a–d** and **8a–d**.

Polymer	$\lambda_{\text{max,abs}}$ in HFIP/nm	$\lambda_{\text{max, PL}}$ in HFIP/nm	$E_g{}^a$/eV	$\lambda_{\text{max,abs}}$ in solid state/nm	$\lambda_{\text{max, PL}}$ in solid state/nm	$E_g{}^b$/eV
7a	331.0	—	3.23	364.5	461.5	2.94
7b	331.5	—	3.23	360.0	456.0	2.96
7c	330.5	—	3.23	372.5	459.0	2.94
7d	329.5	—	3.23	371.5	454.0	2.99
8a	338.0	488.5	3.15	377.5	463.5	2.72
8b	346.0	490.0	3.08	382.5	469.0	2.68
8c	353.0	488.0	3.04	395.0	470.0	2.66
8d	358.5	487.5	3.03	406.5	473.5	2.66
9c[c]	361.0	488.5	3.01	409.0	473.0	2.67

[a] Band gap energy calculated from UV-vis spectra in solution.
[b] Band gap energy calculated from UV-vis spectra in solid state.
[c] Previously reported data [20].

The solid state UV-vis spectra of polymers **7a–d** showed absorption maxima at 360.0–372.5 nm. In the PL spectra of polymers **7a–d** in the solid state with excitation at 360.0–372.5 nm, peak maxima were observed at 454.0–461.5 nm with blue emission, the Stokes shifts being 82.5–97 nm. Band gap energies (E_g), estimated from the extrapolated UV-vis absorption edges in solution and in the solid state, were 3.23 eV and 2.94–2.99 eV, respectively. The E_g values in solution are higher than those in the solid state. This is perhaps due to intermolecular aggregation effects in the solid state [25]. The peak positions of UV-vis and PL spectra in polymers **7a–d** were seen at lower wavelengths than those in the analogous 4,4′-DBTD-containing polymers **9a–d**. By contrast the E_g values, both in solution and in the solid state, for polymers **7a–d** are higher than those of the corresponding polymers **9a–d**. This is because the 4,4′-DBTD unit has a more conjugated structure than the 3,3′-DBTD unit.

In the UV-vis spectra of copolymers **8a–d** in HFIP solution and in the solid state, absorption peak maxima were observed at 338–358.5 nm and 377.5–406.5 nm, respectively, shifted to shorter wavelengths with the increase of 3,3′-DBTD content. The peak positions of the PL spectra of copolymers **8a–d** in the solid state were also shifted to shorter wavelengths with increasing content of 3,3′-DBTD unit, but the solution PL spectra of copolymers **8a–d** hardly changed and were independent of the 3,3′-DBTD content; the peak maxima were almost the same as for the homopolymer **9c**. This might be related to the absence of PL emission in the homopolymer **7c** composed of the 3,3′-DBTD unit. The Stokes shifts were 129.0–150.5 nm in the solutions and 67.0–86.5 nm in the solid state. The E_g values of copolymers **8a–d** (3.03–3.15 eV in solution and 2.66–2.72 eV in the solid state) increased with the increase of 3,3′-DBTD content; the values increased in the 3,3′-DBTD-rich copolymers. The solution UV-vis and the solid state PL spectra for polymers **7c**, **9c** and **8a–d** are shown in figures 7 and 8. In table 4 the spectral data for polymers **7a–d** and **8a–d**, in HFIP solutions and in the solid state, are tabulated together with those for polymer **9c**.

From these results, it is suggested that the disubstituted positions of the undecamethyleneoxy chain on the benzene ring of the DBTD affects the optical properties of polyesters **7a–d**, **8a–d** and **9a–d** composed of the 3,3′- and/or 4,4′-DBTD units, because of its electron-donating effect and the conjugated structures of DBTD, as with the previously reported semi-rigid polyesters comprising the DPTD moiety.

The authors thank Ms Michiko Egawa for her help in obtaining elemental analysis data.

References

[1] Shirota, Y., 2000, *J. mater. Chem.*, **10,** 1.

[2] Hudson, A. J., and Weaver, M. S., 2000, *Functional Organic and Polymeric Materials*, edited by T. H. Richardson (Chichester: John Wily), p. 365.

[3] Adachi, C., Tsutsui, T., and Saito, S., 1990, *Appl. Phys., Lett.*, **56,** 798.

[4] Kukhta, A., Kolesnik, E., Taoubi, M., Drozdova, D., and Prokopchuk, N., 2000, *Synth. Met.*, **119,** 129.

[5] Pei, Q., and Yang, Y., 1995, *Chem. Mater.*, **7,** 1568.

[6] Huang, W., Yu, W.-L., Meng, H., Pei, J., and Li, S. F. Y., 1998, *Chem. Mater.*, **10,** 3340.

[7] Peng, Z., and Zhang, J., 1999, *Synth. Met.*, **105,** 73.

[8] Sato, M., Yamauchi, K., Handa, M., and Kasuga, K., 2000, *Macromol. rapid Commun.*, **21,** 1234.

[9] Sato, M., Nakamoto, Y., Yonetake, K., and Kido, J., 2002, *Polym. J.*, **34,** 601.

[10] Sato, M., Nakamoto, Y., and Tanino, N., 2002, *Polym. J.*, **34,** 158.

[11] Ober, C. K., Jin, J.-I., Zhou, G.-F., and Lenz, R. W., 1984, *Adv. polym. Sci.*, **59,** 102.

[12] Cai, R., Preston, J., and Samulski, E. T., 1992, *Macromolecules*, **25,** 563.

[13] Demus, D., Goodby, J., Gray, G. W., Spiess, H.-W. and Vill, V. (editors), 1998, *Handbook of Liquid Crystals*, Vol. 3 (Weinheim: Wiley-VCH).

[14] Chapoy, L. L. (editor), 1985, *Recent Advances in Liquid Crystalline Polymers* (London: Elsevier Applied Science).

[15] Sato, M., and Nakashima, S., unpublished results.

[16] Sato, M., 1999, *Macromol. Rapid Commun.*, **20,** 77.

[17] Sato, M., Yoshinaga, T., and Koide, N., 2000, *Polym. J.*, **32,** 753.

[18] Sato, M., and Uemoto, Y., 2000, *Macromol. rapid Commun.*, **21,** 1220.

[19] Sato, M., Nakashima, S., and Uemoto, Y., 2003, *J. polym. Sci., A, polym., Chem.*, **41,** 2676.

[20] Sato, M., Notsu, M., Nakashima, S., and Uemoto, Y., 2001, *Macromol. rapid Commun.*, **22,** 681.

[21] Sato, M., and Kitani, Y., 2003, *Liq. Cryst.*, **30,** 1109.

[22] Sato, M., Ohta, R., Handa, M., and Kasuga, K., 2002, *Liq. Cryst.*, **29,** 1441.

[23] Sato, M., and Ujiie, S., 1996, *Adv. Mater.*, **8,** 567.

[24] Sato, M., Ishii, R., Nakashima, S., Yonetake, K., and Kido, J., 2001, *Liq. Cryst.*, **28,** 1211.

[25] Conwell, E., 1997, *Trends polym. Sci.*, **7,** 218.